Chapter 13

A Nanobody-Based Approach to Amyloid Diseases, the Gelsolin Case Study

Adriaan Verhelle and Jan Gettemans

Additional information is available at the end of the chapter

http://dx.doi.org/10.5772/63981

Abstract

Gelsolin amyloidosis (AGel) is an autosomal-dominant inherited disease caused by point mutations in the gelsolin gene. At the protein level, these mutations result in the loss of a Ca^{2+}-binding site, crucial for the correct folding and function. In the trans-Golgi network, this mutant plasma gelsolin is cleaved by furin, giving rise to a 68 kDa C-terminal fragment. When secreted in the extracellular matrix, this fragment undergoes proteolysis by MT1-MMP–like proteases, resulting in the production of 8 and 5 kDa amyloidogenic peptides. Nanobodies, the variable part of the heavy chain of heavy-chain antibodies, have been used as molecular chaperones for mutant plasma gelsolin and the 68 kDa C-terminal fragment in an attempt to inhibit their pathogenic proteolysis. Furthermore, these nanobodies have also been tested and applied as a ^{99m}Tc-based imaging agent in the gelsolin amyloidosis mouse model.

Keywords: AGel, Gelsolin, Nanobody, SPECT/CT, VHH, FAF

1. Introduction

Gelsolin amyloidosis is an autosomal-dominant inherited disease caused by a point mutation in the gelsolin gene; G640A and G640T are most common; G580A and C633A were more recently discovered [1–3]. At the protein level, these mutations result in the amino acid substitutions D187N, D187Y, G167R and N184K in gelsolin domain 2. Consequently, a Ca^{2+}-binding site, crucial for the correct folding and function, is lost. As a result, mutant plasma gelsolin (PG*) adopts an intermediate state between active and inactive, thereby negatively influencing the overall structural stability of the protein and exposing a cryptic, otherwise buried, furin cleavage

site [4]. In the trans-Golgi network, this intermediate form of mutant plasma gelsolin is susceptible to furin cleavage, giving rise to a 68 kDa C-terminal fragment (C68) [5]. In its turn, C68 is cleaved by MT1-MMP–like proteases during secretion into the extracellular matrix. This MMP activity results in the formation of 8 and 5 kDa amyloidogenic peptides, which polymerize into mature amyloid fibrils [6]. Patients are generally heterozygous for the mutations and experience a triad of neurological, ophthalmological and dermatological symptoms starting from their thirties [7]. Given the importance of furin and MT1-MMP–like proteases in cell homeostasis, a classical small compound therapy targeting these proteases is unlikely to be successful. Moreover, the gain-of-toxicity nature of this disease rules out replacement gene therapy. In gelsolin amyloidosis, the mutant gelsolin gene still undergoes normal expression. Curing gelsolin amyloidosis through gene therapy would therefore require the deletion of the mutant gene from every single cell. This is (at the moment) not possible with the available gene therapy technology. Shielding the mutant gelsolin from furin and MT1-MMP–like proteases, however, proved to be a worthwhile approach to tackle this disease. One of that may be applicable to other similar amyloid diseases.

Using nanobodies, the variable part of the heavy chain of heavy-chain antibodies, two routes to address AGel have been explored. In a first approach, nanobodies, which partly protect C68 against MT1-MMP, were intraperitoneally injected in AGel mice [8]. In a second approach, a mouse model expressing Nb11 was developed [9]. Nb11 binds to mutant plasma gelsolin (PG*) and shields it from furin degradation. The mouse model secretes this nanobody in its bloodstream. These mice were crossed with AGel mice. During the secretion pathway, Nb11 encounters PG* in the trans-Golgi network. Both techniques resulted in a reduced deposition of amyloidogenic gelsolin.

The nanobodies binding to C68 are also capable of recognizing the 8 kDa amyloidogenic fragment. This characteristic was further explored to develop a ^{99m}Tc-based imaging agent.

2. Gelsolin amyloidosis

2.1. Discovery

In 1969, the Finnish ophthalmologist Jouko Meretoja [10] first described a new familial amyloidosis syndrome characterized by corneal dystrophy, cranial neuropathies and skin affliction. Over the years, this syndrome came to be known under many different names: Meretoja's disease, amyloid polyneuropathy type IV, gelsolin-related amyloidosis, familial amyloidosis of the Finnish type (FAF), corneal lattice dystrophy type II and gelsolin amyloidosis (AGel).

It was not until 1990 that the role of gelsolin in AGel was demonstrated. Two independent research groups had isolated and sequenced the amyloid fibrils from patient tissues [11, 12]. The fragments appeared to be an internal part of a gelsolin variant having an aspartate to asparagine mutation at position 187 of the primary structure of gelsolin. AGel therefore seemed to arise from an abnormal internal degradation from this gelsolin variant.

In the following years, the role of gelsolin, the genetic cause and pathogenic pathway were further elaborated. At the moment, there are four known mutations, which cause gelsolin-related amyloidosis: D187N, D187Y, G167R and the recently discovered N184K [1–3].

2.2. Biochemistry and genetics of gelsolin

The gelsolin superfamily of actin-binding proteins comprises gelsolin, villin, supervillin, advillin, villin-like protein, severin, fragmin CapG (gCap39) and flightless I [13–16]. These proteins are highly conserved in the animal kingdom, and all contain three or more prototypical 'gelsolin-like' domains. A 'gelsolin-like' domain consists of five or six beta-sheets packed between a long roughly parallel and a short roughly perpendicular alpha helix [17, 18].

Gelsolin was described in 1979 as a protein able to transform solid actin gels into a soluble solution: the gel-sol reaction, hence the name. Present in almost every human tissue, gelsolin is capable of binding, severing and capping actin filaments and plays a pivotal role in cytoskeletal homeostasis [19]. It comes in three isoforms, all derived from the same gelsolin gene located at chromosome 9q34. Alternative splicing gives rise to cytoplasmic gelsolin (CG, 82 kDa), plasma gelsolin (PG, 84 kDa) and gelsolin-3 (82 kDa). The first two are the main isoforms, with PG differing from CG by a 24 amino acid, N-terminal extension, which remains present after cleavage of the signal sequence, and the presence of a disulfide bond. The third variant has only been detected in brain oligodendrocytes, lungs and testis tissue and is characterized by 11 additional residues at the N-terminus [20].

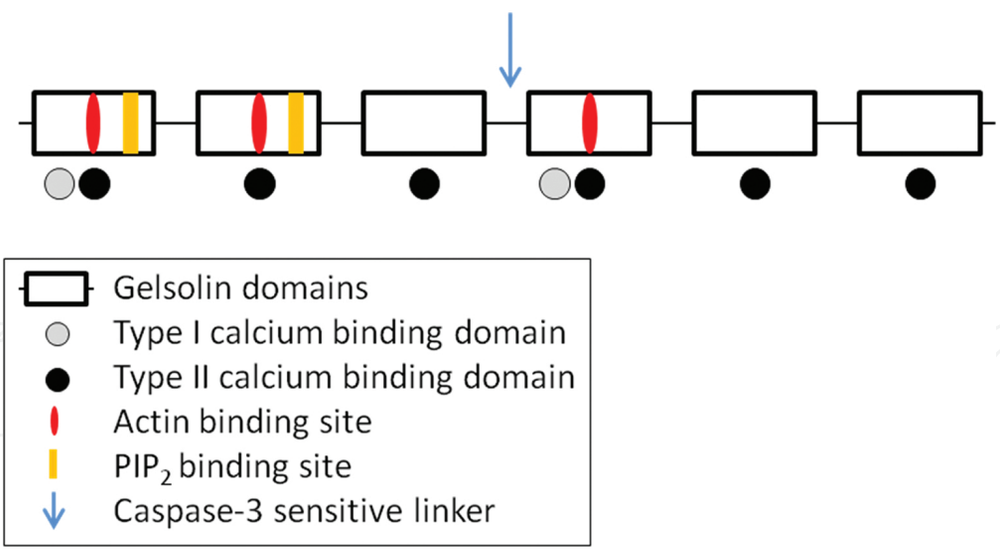

Figure 1. Schematic representation of gelsolin. Black boxes represent the six gelsolin domains. Calcium-binding sites (grey and black dots), actin-binding sites (red), PIP_2-binding sites (yellow) and caspase-3–sensitive linker (blue arrow) are indicated.

Gelsolin is composed of six domains (G1–6) of 120–130 amino acids which, in a calcium-free environment, are closely packed together. This inactive state is controlled by three latches: the tail latch, formed by the C-terminus and G2 domain, the G1–G3 latch and the G4–G6 latch [21].

Upon binding of calcium, the three latches open up and expose the actin-binding surfaces of domains 2, 1 and 4, respectively. Following this activation, gelsolin will bind and subsequently sever F-actin [4]. The sequence homology between G1–3 and G4–6 suggests that the protein arose from a gene triplication followed by a duplication [22]. The two homologous halves are connected through a caspase-3–sensitive linker (**Figure 1**). Overall, stability and function of gelsolin are regulated through Ca^{2+} and phosphatidylinositol 4,5-biphosphate (PIP_2). Each domain contains a Ca^{2+}-binding site, and G1 and G2 also have PIP_2-binding capacity (**Figure 1**) [14].

The G2 domain has two major foci of stability. First, there is the Ca^{2+}-binding pocket (Kd 650 nM) formed by residues D187, E209 and D259 [23]. Second, L166, Q164, N184 and D187 form cooperative hydrogen bonds with one another [18]. Mutation of any of these residues leads to a destabilization of G2 and consequently of gelsolin as a whole. This is actually what happens in AGel. Three out of four of the known mutations (D187N, D187Y and N184K) can be directly traced back to one of these two foci of stability. The fourth mutation, G167R, possibly has a destabilizing effect on hydrogen bonding as it is close to Q164. It should be noted that both the N184K and G167R mutations have only recently been discovered in two isolated patients and their kindred [2, 3]. The overall majority of patients carry the D187N/Y mutation, but it is nevertheless noteworthy to observe that these pathological mutations are all in G2 of gelsolin, pointing to this region as a gelsolin stability sensor.

Although the causative mutations of AGel are present in all three gelsolin isoforms, the plasma variant is the sole source of gelsolin amyloidogenic peptides [24]. As mentioned earlier, the overall stability of gelsolin is highly regulated by Ca^{2+} binding. The AGel mutant plasma gelsolin form can no longer properly bind Ca^{2+} through its G2 domain. Consequently, this aberrant variant gives rise to a structurally intermediate state between active and inactive. This exposes an otherwise internal inaccessible furin cleavage site (R-X-X-R) at the surface of gelsolin.

Furin is a membrane-bound member of the proprotein convertase family, active in the endosomal and lysosomal pathways. It shuttles between the trans-Golgi network and the cell surface while activating a wide range of serum proteins, hormones and receptors [25–27]. During secretion, PG naturally encounters furin without any consequence since wild-type gelsolin is already correctly folded due to high calcium levels in the ER/Golgi compartments. PG* on the other hand is susceptible to pathological furin processing due to its induced structural intermediate state. The scissile bond between R172 and A173 is cleaved, thereby releasing a 68 kDa C-terminal fragment [28]. During secretion, this aberrant C68 constitutes a substrate for MT1-MMP–like proteases present in the extracellular matrix. MT1-MMP–like proteases are members of the matrix metalloprotease family [29]. They play a pivotal role in protein degradation processes during embryonic development and tissue remodelling. Here, however, 8 kDa (AA 173–243) and 5 kDa (AA 173–225) gelsolin amyloidogenic peptides are generated (**Figure 2**). Over time, the 8 and 5 kDa fragments start to aggregate in a cross-beta sheet configuration, a hallmark of amyloid fibrils with the former being the major component of gelsolin amyloid in patients.

http://dx.doi.org/10.5772/63981

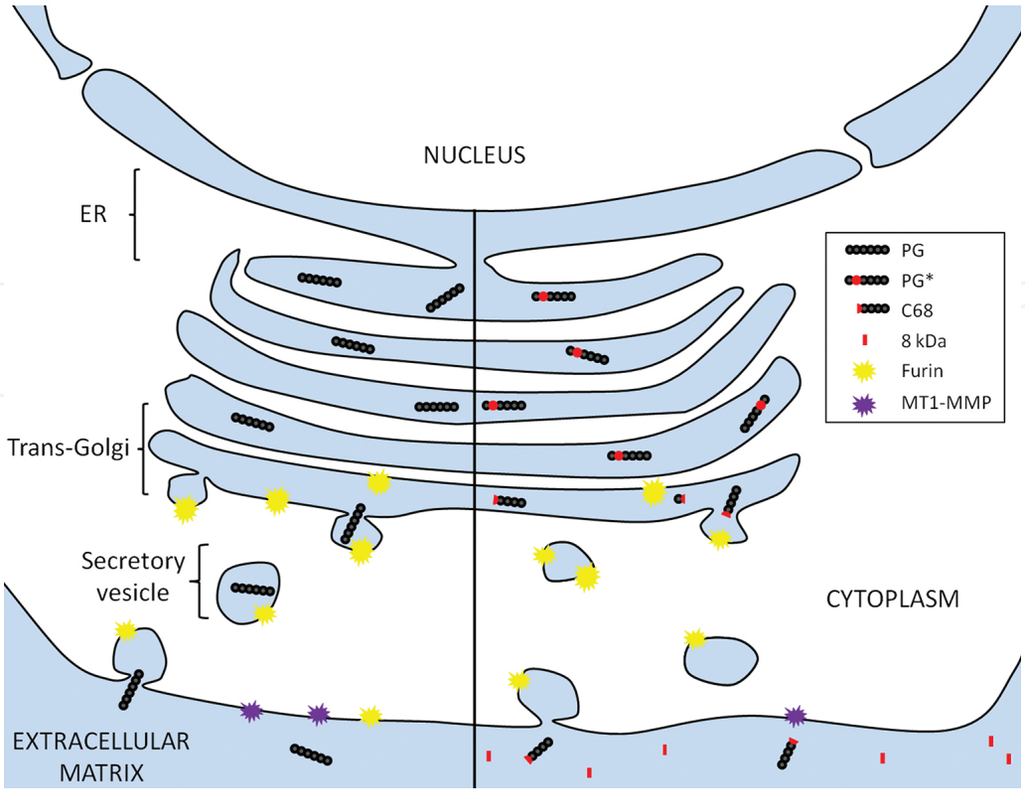

Figure 2. Molecular characteristics of AGel: non-pathological versus pathological plasma gelsolin processing. The left-hand side depicts the non-pathological synthesis and secretion of wild-type plasma gelsolin through the ER and Golgi-network. On the right hand, the mechanism for mutant plasma gelsolin is depicted. Furin cleaves PG* in the trans-Golgi network, thereby releasing a C68 fragment. During secretion, C68 is cleaved by MT1-MMP–like proteases, forming 8 and 5 kDa amyloidogenic fragments in the extracellular matrix.

2.3. Diagnosis and treatment

The clinical diagnosis of AGel most commonly starts with the detection of corneal lattice dystrophy [30]. Together with cutis laxis and bilateral facial pareses, it forms a triad of consistent features differentiating AGel from other amyloid disorders. The diagnosis can be easily confirmed using molecular genetics. In older or homozygous patients, renal amyloidosis, resulting in proteinuria, can also be a first clue [7].

No specific treatment is currently available. Only symptomatic treatments are being offered to improve the overall quality of life. Most important is good ophthalmological care ranging from eye drops to corneal transplantation. Next to that, aesthetic surgery is often needed to ameliorate the patients' overall confidence as the facial pareses and cutis laxis burden the patients with a constant droopy facial expression [31].

Although therapeutic strategies involving the inhibition of protease activity have been suggested, unwanted side effects are to be expected given the major physiological roles of furin and MT1-MMP [28, 29]. Tackling the problem the other way round, directly shielding PG* from degradation, may prove to be a more valuable route, as will be discussed later in this chapter.

2.4. A gelsolin amyloidosis mouse model

To further study the molecular aspects of the disease and to test the different therapeutic avenues, two animal models were set up. In a first attempt, the gene coding for the 8 kDa amyloidogenic fragment was successfully transferred into the genome of *Drosophila melanogaster*. Unfortunately, AGel amyloid deposition could not be detected [7].

As of 2009, a mouse model is available that faithfully recapitulates the entire proteolytic cascade of human PG* [32]. Following the electroporation of the human plasma GSN cDNA, carrying the D187N mutation, into mouse ES cells, a transgenic animal was obtained where gelsolin is expressed under control of a muscle creatine kinase (MCK) promoter. PG*, C68 and the 8 and 5 kDa amyloidogenic fragments were detected in the heart, skeletal muscle, diaphragm and skin. Plasma samples contain both full length PG* and C68. With age, increasing amounts of gelsolin-positive amyloid depositions can be seen in the endomysium. Eventually, the phenotype of old homozygous D187N mice starts to resemble sporadic inclusion body myositis (sIBM) with accompanied muscle weakness.

3. Nanobodies

3.1. Research and clinic applications of conventional antibodies

Since the introduction of hybridoma technology in 1975, monoclonal antibodies (mAb) have become an indispensable tool in fundamental research and all sorts of clinical applications [33]. The ability to mass produce antibodies against a plethora of proteins, carbohydrates, nucleic acids and haptens gave rise to molecular diagnostic tests, such as ELISA, Western blotting, immunohistochemistry (IHC) and immunofluorescence. Antibodies in the clinic are used in diagnostic applications by linkage to radioactive or fluorescent moieties. Furthermore, they are also being applied therapeutically, be it directly or as a route for drug delivery. As the applications became more and more sophisticated and diversified, the potential pitfalls of this technology also surfaced. First, the production of vast amounts of mAbs is very expensive. Second, the mAb format is hard to manipulate to obtain site-specific linkage to other molecules such as fluorophores and radioactive nuclides. Last but not least, mAb hold the potential of evoking an immune response rendering the therapy ineffective. This last hurdle has been addressed with the production of so-called humanized antibodies. These second-generation antibodies contain a humanized antigen-binding fragment (Fab). Third-generation antibodies go one step further and also include an engineered Fc domain to improve the therapeutic activity in patients, particularly in subpopulations expressing low affinity variants of the Fc receptor [34].

Conventional antibodies are comprised of 2 heavy chains and 2 light chains. This multichain nature is one of the major hurdles when trying to manipulate mAb. Attempts have been made to bypass this by producing mAb fragments such as antigen-binding fragments and single-chain variable fragments (scFv). The first, Fab, is composed of the variable and constant domain of a heavy chain, combined with the variable and constant domain of a light chain. The second,

http://dx.doi.org/10.5772/63981

scFv, only contains the variable parts of the heavy and light chain, but these are interconnected through a linker. Although these smaller formats ameliorated some of the problems posed by classical mAbs, their production still proved to be troublesome and the functionality of the original mAb was (partly) lost in some cases.

3.2. Discovery of nanobodies

By a stroke of luck in 1993, a new type of antibody was discovered in the blood of Camelus dromedarius [35]. These antibodies consist solely of two heavy chains; hence, they were named heavy-chain antibodies (HCAbs). Their paratope is no longer formed by a combination of a heavy and light chain variable fragment but consists exclusively of the variable fragment of a heavy chain. The single-domain nature of this paratope offered the natural solution for which researchers had been looking for. It has since been named variable domain of the heavy chain of heavy-chain antibodies, VHH in short or Nanobody® (www.ablynx.com) (**Figure 3**). Since their discovery, these HCAbs have been detected in the blood of all Camelidae family members, nurse sharks, wobbegongs and ratfish.

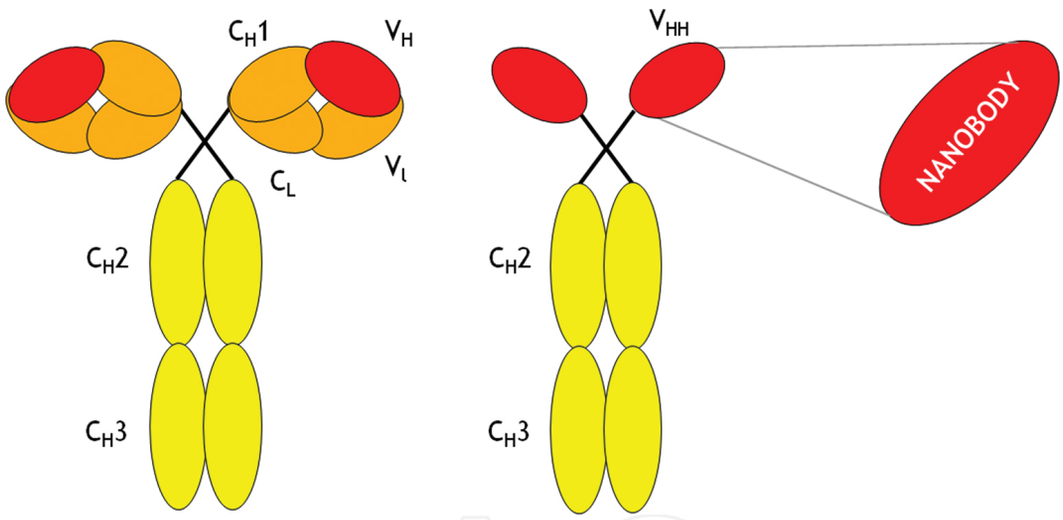

Figure 3. Schematic representation of a conventional antibody, heavy-chain antibody and a nanobody. A conventional antibody (left) consists of two heavy chains (C_H3, C_H2, C_H1 and V_H) and two light chains (C_L and V_l). Heavy-chain antibodies (middle) only consist of two heavy chains (C_H3, C_H2 and V_{HH}). A nanobody (right) corresponds with the variable part of the heavy chain of heavy-chain antibodies (V_{HH}).

3.3. Properties and production of nanobodies

The most important novelty about nanobodies was, and still is, the fact that they are the smallest, single-domain, natural, antigen-binding fragment available. Their complementary determining regions 3 (CDR3) sequences are on average longer (16–18 AA) compared those of regular human antibodies (12 AA). Not only does this compensate for the absence of a light chain, but it also allows the CDR3 to form protruding loops that are able to bind cryptic epitopes. The fact that they are encoded by a single short gene fragments allows easy and straightforward protein engineering, thereby overcoming one of the mayor hurdles of the

multichain nature of conventional Abs. By the same token, it allows relatively easy production in bacteria and yeast cells. With yields of up to 40–70 mg/l, nanobodies can be produced at a fraction of the cost of mAbs. When produced, their high resistance towards chaotropic reagents or prolonged high temperatures and stability at high concentrations allows easy storage without any functionality loss.

3.4. Nanobody applications

Nanobodies, being small and stable, are ideal candidates for various research purposes, diagnostic or clinical applications. Equipped with a radionuclide, they can be applied as imaging tracers in a single-photon emission computed tomography (SPECT) or positron emission tomography (PET)-based set-up allowing in vivo visualization of tumours, atherosclerotic plaques and rheumatoid arthritis-associated inflammation sites [36–38]. Nanobodies are also capable of stabilizing proteins in a particular conformation and of minimizing structural flexibility. This has been nicely demonstrated in the case of human lysozyme amyloidosis, a hereditary systemic disease associated with at least seven amyloidogenic lysozyme variants [39, 40]. Aggregation of these lysozyme variants leads to the accumulation of amyloid in the extracellular matrix of several tissues and organs. Two nanobodies have been identified who, upon binding mutant amyloidogenic lysozyme (D67H and I56T), restored the global cooperativity characteristics of the wild-type protein through direct contact and long-range conformational effects. What's more, this stabilizing capacity can also be conducive to crystallizing proteins. β2-microglobulin–specific nanobodies have been shown to serve as efficient crystallization chaperones for transient intermediate species during fibrillation [41]. This type of antibody chaperone co-crystallization was also used to unravel the structure of the G protein-coupled receptor β-2 adrenergic receptor (β2AR), research which received the 2012 Nobel Prize in Chemistry [42].

Another major field where the potential use of nanobodies is currently being explored is amyloidosis. In Alzheimer's research, nanobodies have been found which inhibit beta-secretase 1 (BACE1) activity, the first step in amyloid beta formation, both in vitro and in vivo [43]. Alternatively, nanobodies could also be raised against amyloid precursor protein (APP) to protect it from BACE1 degradation, as direct inhibition of the enzyme could evoke unwanted side effects. We present here the case of gelsolin amyloidosis where this approach has proven successful both in vitro and in vivo. The remainder of this chapter will focus on the obtained results, current status and future prospects regarding this AGel research arena.

4. Extracellular targeting of the AGel pathological pathway

Consecutive aberrant cleavage of PG* by furin and MT1-MMP–like proteases leads to the production of amyloidogenic fragments which eventually polymerize into fibrils, causing gelsolin amyloidosis pathology. But these two proteases are active in different compartments. Indeed, whereas furin is active in the (intracellular) ER-Golgi compartments, MT1-MMP is inserted in the plasma membrane and oriented to the extracellular environment. This

http://dx.doi.org/10.5772/63981

has far-reaching consequences in terms of molecular therapeutic avenues that should be followed when gelsolin has to be protected from cleavage by either of these proteases. As the second cleavage step occurs in the extracellular matrix, we reasoned that it might be possible to block this process by intraperitoneal administration of C68 chaperone nanobodies [8].

A dromedary was simultaneously immunized with the G2 domain and the 8 kDa fragment of PG*. Phage panning was also performed with both gelsolin fragments. This yielded three different nanobodies, termed FAF Nb1-3. All three bind to PG, PG*, C68 and the 8 kDa peptide

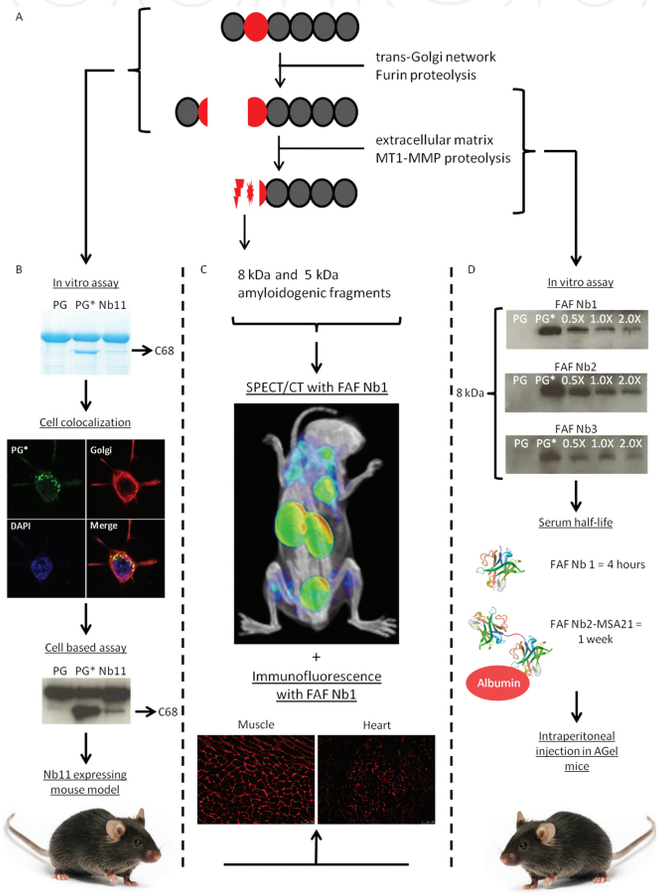

Figure 4. Overview of different nanobody-based strategies to diagnose and to counter amyloidogenesis in transgenic mice. A, Schematic representation of the steps leading from mutant plasma gelsolin to the 8 and 5 kDa amyloidogenic fragments. B (upper panel), Gelsolin Nb11 reduces C68 formation in vitro—lane 1: PG incubated with furin, lane 2: PG* incubated with furin and lane 3: PG* incubated with furin and Nb11. B (second panel), Nb11 co-localizes with mutant gelsolin in the secretory pathway of HEK293T cells. B (third panel), **Nb 11** decreases C68 formation in HEK293T cells: lane 1: medium from cells transfected with PG, lane 2: medium from cells transfected with PG* and lane 3: medium from cells transfected with PG* and Nb11. This led to designing the Nb11-expressing mouse model. C, Representative images obtained with ^{99m}Tc-labeled FAF Nb1 in 9-month-old AGel mice. The heart and front and hind leg muscles show a clear signal (blue). Kidneys and bladder signal represents unbound nanobody which is cleared through the urinary system (green and red). FAF Nb1 can also be used as a primary antibody to stain amyloidogenic gelsolin build-up in AGel mice tissue (lower panel). D (upper panel), FAF Nb1-3 partly inhibits C68 proteolysis in vitro. For each nanobody, from left till right, after incubation with MT1-MMP: PG, PG*, PG* + 0.5, 1.0 and 2.0 X FAF Nb. Numbers indicate the Nb/PG* molar ratios. D (middle panel), Linkage with the albumin-binding MSA21 nanobody increases serum half-life from 4 h to more than 1 week (middle panel). D (lower panel), In vivo analysis was performed through intraperitoneal injection in AGel mice.

when tested through immunoprecipitation on crude bacterial lysates, but they did not cross-react with CapG, a protein that is structurally related to gelsolin. Unlike gelsolin, CapG is only capable of capping actin filaments but does not sever. It is the member of the gelsolin superfamily most closely resembling gelsolin. It possesses 49% identity with the N-terminal half of gelsolin.

The hypothesis was that if one of these FAF nanobodies bound to C68 in the vicinity of the MT1-MMP cleavage site or an important docking area, it would be able to (at least partly) inhibit the production of the 8 kDa fragments. This was indeed confirmed by in vitro experiments. C68 was preincubated with one of the three FAF Nbs after which MT1-MMP was added to the mixture. Formation of the 8 kDa fragment could be followed by Western blotting, and this showed a 70–80% reduction in the presence of a FAF nanobody, attesting to their ability to indirectly prevent MT1-MMP activity on gelsolin (**Figure 4A** and **D**). Nb13, a nanobody that binds to the linker between gelsolin domains 4 and 5, did not show the same effect. Furthermore, the FAF Nbs had no effect on the proteolysis of collagen, another substrate of MT1-MMP. Therefore, it was concluded that a nanobody can be used as a chaperone to prevent degradation of a structural protein by an enzyme without directly inhibiting the activity of the enzyme. In doing so, potential side effects may be prevented. Whether the observed effects are due to a direct inhibition of MT1-MMP docking on C68 or shielding the cleavage site or rather due to an indirect structural affect caused by the binding of the Nb with C68 still remains to be clarified. A crystal structure of MT1-MMP bound to C68 would bring clarity in this matter.

While these results were promising at first, a new caveat presented itself when considering that nanobodies, because of their small size, are characterized by rapid blood clearance. This could impede their use as a therapeutic in vivo. Indeed, although their small size is mostly advantageous, when used as a therapeutic, it is rather a burden. Thus, it seemed necessary to increase their half-life in the circulation as this will improve their probability of binding C68 gelsolin. To achieve this goal, FAF Nb1-3 were coupled to the albumin-binding nanobody MSA21 through a short Gly-Ser linker. This linkage did not greatly affect the binding affinity between the Nb and C68 (FAF2 = Kd: $8.4 \times 10^{-7} \pm 4.7 \times 10^{-8}$ M, FAF2-MSA21 = Kd: $5.4 \times 10^{-7} \pm 0.6 \times 10^{-7}$ M, determined by isothermal titration calorimetry). The bispecific FAF2-MSA21 Nb binds albumin in the bloodstream, and the formation of this larger complex should extend the half-life, resulting in a higher efficiency of the FAF Nb1-3 therapeutic intervention. Serum analysis of injected mice confirmed this assumption. While the monovalent FAF Nb1-3 were no longer detectable after 4 h, the bispecific format could still be clearly visualized up until one week post-injection (**Figure 4D**). Additionally, the linkage between FAFNb1-3 and MSA21 did not offset the MT1-MMP–inhibiting potential in vitro. Hence, all requirements were fulfilled to test their effect in vivo.

The in vitro results were validated using the available AGel mouse model. Over a period of 12 weeks, mice were weekly injected with 100 μg of either FAF Nb1, FAF Nb2-MSA21 or phosphate-buffered saline (PBS). The trial started at the age of 4 weeks, and the nanobodies used were the ones which performed best during the in vitro set-up. End-stage analysis consisted of immunohistochemistry (IHC) and ex vivo muscle contractility measurements. IHC revealed a decrease in amyloidogenic gelsolin staining for FAF Nb1 of 15% and FAF Nb2-

MSA21 of 30%. Both results were statistically significant. The difference between both nanobody formats shows that a longer half-life is definitely desirable in a therapeutic approach such as this. The reduction seen with IHC in the FAF Nb2-MSA21–treated mice translated into improved muscle contractility and relaxation speed function in the extensor digitorum longus (EDL). Therefore, these nanobodies are endowed with a therapeutic quality. It should be noted that the FAF Nbs display an intermediate affinity for their target. Although clear data in support of this contention are wanting, it seems likely that stronger binders might even have stronger effects in vivo. Further exploration of the FAF Nb2-MSA21 potential in human gelsolin amyloidosis patients requires two important modification to be made. Firstly, the MSA21 nanobody would have to be replaced by a human serum albumin binder. The longer serum half-life of human versus mouse albumin (19 days versus 35 h) may further lower the administration frequency. Secondly, although nanobodies are known for their low immunogenicity, humanizing their framework regions can further decrease the risk of an undesirable immune response during therapeutic intervention. More specifically, a universal humanized nanobody scaffold has already been proposed onto which all the CDR antigen-binding loops could be grafted [44].

5. Intracellular targeting of the AGel pathological pathway

Thanks to their excellent stability, nanobodies are also valuable compounds to be used as intrabodies. The reducing environment of the cytoplasm seems to have little effect on their functionality [45, 46]. As mentioned above, the FAF Nb approach significantly reduced AGel amyloid build-up in vivo, but it did not completely halt the 8 kDa peptide production. AGel pathogenesis is a two step process; a furin cleavage of mutant plasma gelsolin produces C68, which is then on its turn cleaved by MT1-MMP, thereby releasing 8 kDa amyloidogenic peptides. This opens the opportunity for a double-hit approach.

For that reason, we tested whether a different set of gelsolin nanobodies could be applied as a chaperone for gelsolin to divert furin activity in the same manner as we had implemented the FAF Nb1-3 towards C68 [9].

The nanobodies used in this study were not specifically designed for this purpose. Instead, they had been raised against wild-type gelsolin and characterized some time ago. Through in vitro epitope mapping experiments, Nb11 was shown to interact with the G2–G3 domains (N-terminal half), whereas Nb13 interacts with G4–G5 (C-terminal half). Furthermore, both nanobodies interact with different populations of gelsolin in cells. Indeed, Nb11 binds human gelsolin with high affinity ($Kd = 3.65 \times 10^{-9} \pm 0.54 \times 10^{-9}$ M, determined by isothermal titration calorimetry), irrespective of whether calcium is present or not, whereas Nb13 strongly interacts with gelsolin ($Kd = 9.26 \times 10^{-9} \pm 1.61 \times 10^{-9}$ M, determined by isothermal titration calorimetry), only when the latter is activated by calcium. Both nanobodies were further shown to act as reliable tracers of gelsolin in MCF-7 cells when expressed as intrabodies. Both gelsolin and nanobody are abundantly present in the cytoplasm of unstimulated MCF-7 cells, preventing straightforward assessment of their co-localization. However, when the cells were stimulat-

ed with epidermal growth factor (EGF), both endogenous gelsolin and the nanobodies extensively decorated membrane ruffles [47]. In view of the binding region of Nb11 in gelsolin, it was surmised that it could interfere with furin-mediated degradation. In analogy with the MT1-MMP study, these gelsolin nanobodies were incubated with PG*, and Western blotting showed that only Nb11 reduced furin cleavage of PG* by 34% when added in concentrations equimolar to PG* (**Figure 4A** and **B**).

This finding, however, does not guarantee that the same result will be obtained in mammalian cells. Plasma gelsolin will naturally travel through the secretory pathway, but simple expression of the nanobody will result in its cytoplasmic and nuclear localization in cells. Hence, the nanobody will not be able to protect gelsolin. For this reason, the nanobody was equipped with an ER signal peptide to ensure its secretion through the Golgi apparatus. Furin naturally resides in the Golgi apparatus, and the first step in the AGel pathology takes place in this compartment. By quantifying the amount of C68 that is secreted in the extracellular environment, it could be confirmed that Nb11 exerts a protective effect. The cell media from HEK cells transfected with PG* and Nb11 contained 80% less C68 compared to HEK cells solely transfected with PG* (**Figure 4B**).

Although nanobodies can, and are, currently being applied in research involving intracellular perturbation of protein-protein interactions, at the moment there is no efficient, fail proof method to introduce them into cells in a recombinant format. Therefore, to test whether the observed effect of Nb11 in vitro could be reproduced in vivo, a Nb11-expressing mouse model had to be created. To our knowledge, this is the first transgenic mammal that contains a therapeutic nanobody in its genome. The ER-directed Nb11 cDNA was cloned in the pROSA-DV2 vector, which targets the ROSA26 locus. This locus was identified in 1991 using gene-trap mutagenesis screening on embryonic stem cells. Thanks to its ubiquitous expression in both embryonic and adult tissues, over 130 knock-in mouse lines have been created using this cloning site. G4 ES cells were electroporated, and positive colonies were selected through Southern blotting. Next, cells were aggregated with Swiss inner cell mass cells. These blastocysts were transferred into pseudopregnant mice uteri, and the resulting chimeric offspring was backcrossed with wild-type C57BL/6 to check for germline transmission. Finally, these mice could then be crossed with a non-tissue specific Cre/lox-deleter mouse strain. This resulted in CAGG promoter-driven Nb11 expression, resulting in the first Nb11-expressing mice. Nb11 could be visualized and quantified in the serum through co-immunoprecipitation and Western blotting.

The newly developed Nb11 mouse model was crossed with AGel mice. Double positive offspring was evaluated at three distinct time points: 3, 6 and 9 months. Gastrocnemius muscle tissue was stained for AGel build-up. A costaining for laminin was used as an internal control and to discern any potential artefacts. The AGel staining was homogenous in every age group, allowing quantification. Compared to AGel mice or littermates not expressing Nb11, a reduction in AGel staining of 27 and 28%, respectively, could be detected at 3 and 9 months of age. For the group of 6 months, no significant reduction could be found. The reason for this is unclear. The group of 9-month-old mice was also subjected to a muscle performance evaluation. The extensor digitorum longus (EDL) muscle showed a strong attenuation of the typical

decrease in contraction speed during the fatiguing protocol. This therapeutic effect was not mimicked by Nb13 that binds to another region in gelsolin (G4–G5 linker) and that had no effect on gelsolin degradation by furin. Neither Nb11 nor Nb13 showed any cross-reactivity with endogenous mouse gelsolin. Thus, Nb11 attenuates amyloid build-up by (partly) protecting gelsolin against degradation by furin. One might wonder why the reduction in AGel staining was not as high as expected, given that Nb11 is a strong binder (Kd ~ 5 nM) where calcium moreover has no effect on binding. One possibility involves the relative expression levels of gelsolin and Nb11. Western blotting with internal gelsolin and nanobody standards indicated that both are present at roughly equimolar levels. In the AGel mouse model, however, gelsolin is secreted from muscle, whereas nanobody expression is thought to be secreted from multiple organs, tissues and cells, because no tissue-specific promoter was used to drive expression of the nanobody. Therefore, the nanobody that was detected in the serum of these animals has multiple origins suggesting that its secretion from muscle is significantly lower as compared to gelsolin secretion. This contention however needs to be examined experimentally.

6. In vivo visualization of AGel build-up

AGel is a chronic, gain of toxicity, affliction. Accordingly, any therapy will have to be administered throughout the entire lifetime of the patients. It is therefore important, during therapy development, to test promising compounds over a long period of time and assess the effects at different time points during the course of the trial. During the Nb11 experiments, this had to be done by using different groups for every time point since the current methods of AGel analysis are end-stage [8, 9]. Not only does this greatly augment the amount of mice needed, it also makes it impossible to evaluate the drug effect and amyloid build-up in a continuous manner. In the hope of resolving this drawback, we set out to develop a nanobody-based imaging agent. The ultimate goal was to be able to visualize the AGel amyloid build-up in vivo in a non-invasive manner. This would facilitate evaluation of drug responses at different time points over the entire course of treatment in the same animal.

6.1. Labelling of nanobody through ^{99m}Tc linkage to His_6 tag

Thanks to their excellent stability, small size and single-chain nature, nanobodies represent an ideal antibody derived format for transformation into a radionuclide-based amyloid imaging agent. ^{99m}Tc was the radionuclide of choice being readily available and displaying a half-life long enough to allow good quality imaging, but short enough to minimize the overall radiation burden during the trial. Linking it to a nanobody is also a straightforward process. Simply equipping the nanobody with a N- or C-terminal His_6 tag allows chelation with ^{99m}Tc via the tricarbonyl method [48]. Furthermore, ^{99m}Tc is compatible with SPECT, the imaging modality most ideal for visualization in small laboratory animals used during research trials such as this.

FAF Nb1-3 were the prime candidates to be explored for their ability to serve as an imaging tool. When administered as in vivo imaging agents, FAF Nb1-3 are required to remain stable for some time in the complex environment of the blood and extracellular matrix. In a preliminary test phase, FAF Nb1-3 were therefore incubated in C57BL/6 mouse serum at 37°C and found to remain stable for up to 24 h without deterioration.

As a last test before the first in vivo trials, a test labelling was performed. Using instant thin-layer chromatography (ITLC) and reverse-phase high-performance liquid chromatography (RP-HPLC), the radiochemical purities were determined to be 99.7 ± 1.3%, 99.7 ± 0.9% and 98.3 ± 1.0% for FAF Nb1-3, respectively.

6.2. Specificity and background signal determination

One of the key aspects of a good imaging agent is the capability of specifically generating a high signal wherever its target is present without provoking a significant background signal. As discussed earlier, FAF Nb1-3 are capable of binding their target with great specificity in vitro. To test whether this remained true in vivo, a group of 9-month-old WT C57BL/6 mice were injected with ^{99m}Tc-FAF Nb1-3. Nanobody BcII10 against β-lactamase of Bacillus cereus was used as a negative control [49]. SPECT/CT images and dissection analysis revealed the classic high kidney and bladder uptake of renal-filtered small hydrophilic proteins of which nanobodies are a textbook example. All the other organs showed no significant high signal when comparing the FAF Nb1-3 with the BcII10 control. From these data, it can be concluded that the FAF Nb1-3 do not show any nonspecific binding when administered to mice (and they do not cross-react with mouse gelsolin either).

The experiment was repeated in 9-month-old AGel mice (**Figure 4C**). At this age, the animals show considerable gelsolin amyloid build-up in the muscle tissue. Both FAF Nb1 and 2 showed significant uptake in skeletal muscle, heart and diaphragm. In the AGel mouse model, these represent three out of the four tissues in which gelsolin amyloid builds up over time. The fourth, the skin, could not be identified with the FAF Nbs, although it is possible that this organ only becomes affected later in life. Overall, this experiment showed that FAF Nb1-2 are capable of specifically recognizing gelsolin amyloid build-up in the AGel model. FAF Nb3 on the contrary did not seem able to provoke a significant signal in the heart nor diaphragm.

The two experiments described above were used to calculate both a signal-to-noise and a signal-specificity score. The first is defined as the signals gained with FAF Nb1-3 in AGel mice muscle over the signal obtained in AGel mice liver. The latter is defined as the signal gained with FAF Nb1-3 in AGel mice over the signal gained with Nb BcII10 in AGel mice. On both characteristics, FAF Nb1 scored the best. Combined with the fact that it also has a slightly better affinity for the 8 kDa peptide (FAF Nb1: $3.8 \times 10^{-7} \pm 1.2 \times 10^{-8}$ M, FAF Nb2: Kd: $8.4 \times 10^{-7} \pm 4.7 \times 10^{-8}$ M and FAF Nb3: Kd: $6.6 \times 10^{-7} \pm 1.7 \times 10^{-7}$ M, determined by isothermal titration calorimetry), FAF Nb1 was appointed as the best candidate for further development as a AGel ^{99m}Tc-based imaging agent.

http://dx.doi.org/10.5772/63981

6.3. Qualitative and quantitative characteristics

The ultimate goal was to see whether the FAF Nbs could be implemented as imaging tools during the screening of potential AGel therapeutics. This of course means that not only do we want to qualitatively image the amyloid build-up, but we also want the rendered signal to hold quantitative information. Only then would it be possible to track the therapeutic effect in a longitudinal follow-up study.

The intervention study with the gelsolin Nb11-expressing mouse model presented an ideal opportunity to test ^{99m}Tc-FAF Nb1 for any quantitative properties. As stated above, by crossing the Nb11 expressing mice with the AGel mice, we were able to reduce AGel amyloid burden as detected by IHC. The experiment was repeated, but now, starting at the age of 3 months, the mice underwent a SPECT/CT scan with ^{99m}Tc-FAF Nb1 every two months. Two groups were analyzed with IHC: one at 9 months of age and another at 11 months.

In the SPECT/CT images, the signal coming from the heart and hind leg muscle was quantified using AMIDE software. The same size region of interest was used for every animal at every time point. No significant differences could be discerned in the heart tissue. This is not so surprising since IHC had revealed earlier that the heart only seems to be homogeneously affected from the age of 7–9 months onwards. Therefore, a good quantification is not possible before that time. In the muscle tissue, however, the SPECT/CT analysis revealed a significant difference at the age of 7 and 9 months. Why the same was not true at 11 months, further research will have to reveal.

At the end stages of 9 and 11 months, mice were dissected right after SPECT/CT imaging. Signal strengths were determined for hind leg muscle and the heart. The same pattern as with SPECT/CT analysis could be found, a difference at 9 months but not at 11 months. The same tissue also underwent IHC, which still is the golden standard when it comes to amyloid detection and quantification. The IHC analysis confirmed that gelsolin staining in the heart tissue is not yet homogenous so these samples were not quantified. The muscle on the other hand showed good overall staining. Hence, IHC confirmed the result obtained with SPECT/CT imaging and dissection analysis, a significant difference at the age of 9 months but no longer at 11 months.

7. Future prospects

7.1. Combined therapy

Gelsolin amyloidosis is caused by a point substitution in the GSN gene which has a destabilizing effect on the second gelsolin domain. As a result a cryptic, otherwise buried, furin cleavage site is exposed at the surface. The plasma isoform encounters furin along the secretory pathway in the trans-Golgi network, at which point it is cleaved, thereby releasing a 68 kDa C-terminal fragment. In its turn, this C68 fragment is processes by MT1-MMP–like proteases leading to the production of 8 and 5 kDa amyloidogenic fragments.

This two-step pathological process allows intervention at two very distinct levels. The furin section takes place intracellularly, inside the trans-Golgi network, a site which is still quite

troublesome to target with non-small-compound therapeutics. The MT1-MMP section takes place in the extracellular matrix, a region easily accessible through injections.

Both routes were explored, and the results are described above. Although both approaches proved to hold a therapeutic potential, none of them completely solved the AGel pathogenesis. Therefore, the next logical step is to combine them in a single therapeutic format. Once again the single-domain nature of nanobodies came in handy. Using straightforward cloning techniques, FAF Nb1 was linked to the C terminus of Nb11 which contains a secretion signal. The linker between both nanobodies contains a MT1-MMP–sensitive linker. The idea behind the construct is that when expressed the bispecific nanobody will perform its PG* chaperone function in the trans-Golgi network. During secretion, the MT1-MMP–sensitive linker will lure MT1-MMP away from the already lower amount of C68. This process will also release FAF Nb1 from Nb11 in situ, making it available to chaperone C68 and further diminish the overall production of the 8 kDa amyloidogenic pathway (**Figure 5**).

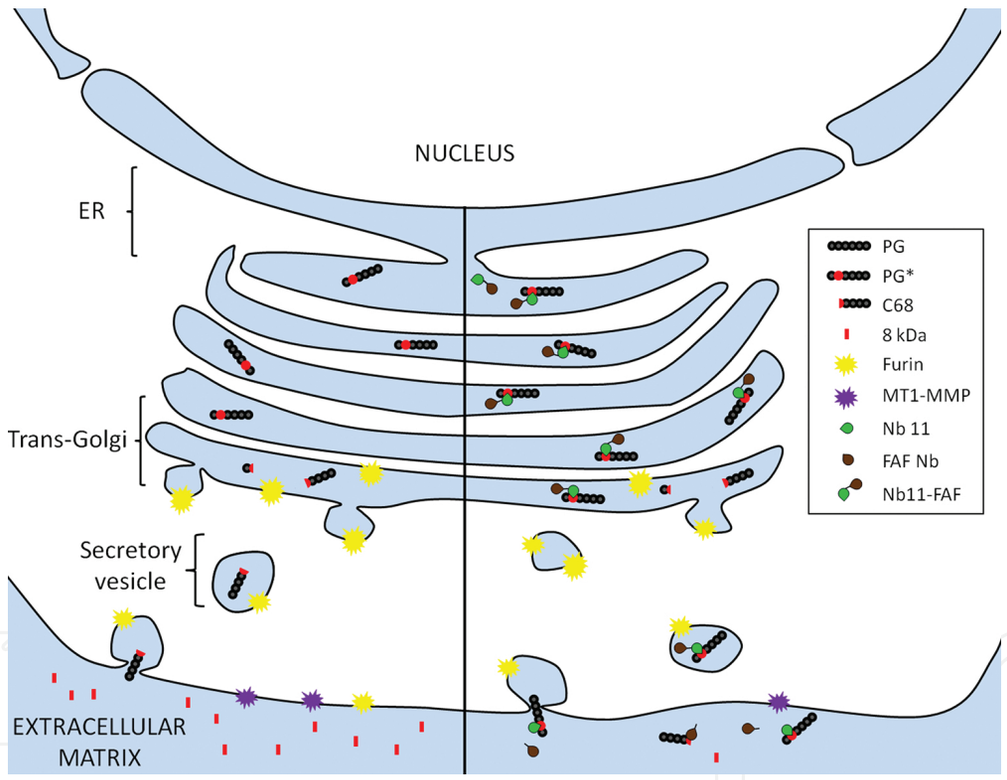

Figure 5. Envisioned molecular mechanism of the therapeutic bispecific Nb11-FAF1. The left-hand side depicts the pathological PG* processing with the formation of C68 in the trans-Golgi network and the 8 and 5 kDa amyloidogenic fragments in the extracellular matrix. On the right-hand side, the intervention with bispecific Nb11-FAF1 is shown. In the trans-Golgi network, the nanobody uses its Nb11 moiety to bind PG* and (partly) protect it from furin degradation. In the extracellular matrix, the MT1-MMP–sensitive linker between Nb11 and FAF1 serves as a decoy. At the same time, FAF Nb1 is released and is able to perform its C68 chaperoning effect, thereby further decreasing the overall formation of 8 and 5 kDa amyloidogenic fragments.

This hypothesis has already been tested in vitro. A combined Furin/MT1-MMP degradation assay was set up. Quantification of the amount of 8 kDa peptide showed Nb11-FAF1 outper-

formed both Nb11 and the individual FAF Nb1-3. Meaning that, in vitro, the double-hit approach shows a synergistic effect compared to the individual therapies.

For in vivo testing, a gene therapy approach could be chosen. Adeno-associated viruses (AAVs) are naturally occurring, non-pathogenic, replication-deficient viruses. They are capable of infecting non-dividing cells and reside in the nucleus under the form of episomal concatemers. This makes them ideal candidates to be used as gene therapy vectors. Their most important downside is the limited packaging capacity of about 5 kb [50]. Given its small size, this should not pose a problem for our Nb11-FAF1 application. Since AGel expression in the transgenic model is driven from muscle, a serotype with a muscle tropism would be preferential.

7.2. Beyond AGel

The studies performed with the AGel mouse model have shown that nanobodies are useful, potent therapeutics for both extra- and intracellular targets. They also highlighted that nanobodies can be used as an imaging tool in AGel, thereby facilitating the screening of potentially new therapeutic compounds. While AGel is an orphan disease, it should be emphasized that this strategy can be extrapolated to other amyloidogenic afflictions. The most infamous type of amyloidosis, Alzheimer's, actually has a quite similar pathogenesis; the sequential proteolysis of Alzheimer's precursor protein by β-secretase and γ-secretase results in the release of Aβ amyloidogenic peptides. Nanobodies against this β-secretase have already proven to be therapeutically active in a transgenic AD mouse model [43]. As already stated earlier, we believe that in the long run, it would prove more beneficial to target the APP instead of the secretases. Inhibiting a protease will most likely provoke unwanted side effects, whereas chaperoning the target, as in the AGel research discussed in this chapter, is more unlikely to do so.

Raising nanobodies against full length APP, s-APP β or Aβ, may result in nanobodies that bind near the β-secretase cleavage or docking site and that block the formation of s-APP β. A double-hit strategy as in the AGel case will most probably be more difficult to achieve. The gamma secretase is a multiunit integral membrane protein. It cleaves transmembrane passes. At the moment, there are no reports of nanobodies being able to integrate into the plasma membrane and remain functional. In addition, gamma secretase proteolysis also takes place in the non-pathogenic processing of APP. As the transmembrane part of C-terminal fragment-alpha and C-terminal fragment-beta is identical, even a chaperone-based intervention may provoke unwanted side effects.

Up until now, we have only discussed preventing the formation of amyloidogenic peptides. But directly targeting the amyloidogenic peptides, after their formation, also holds great therapeutic potential. The deposition of amyloid fibrils is the primary pathological feature of this group of afflictions. In recent years, however, scientific research towards the initial processes leads to fibrillation, implicated that the initial oligomeric aggregates may be the most toxic species in amyloid pathogenesis and mature fibrils may be far less pathogenic than previously thought [51, 52]. These new results hint to new therapeutic strategies. First, one could try to stimulate fibrillation, thus attempting to lower the half-life of small oligomeric

aggregates. Secondly, one could try to remove the amyloidogenic peptides altogether as soon as they are formed. Most likely, the latter will prove to be the most rewarding in the long run. Because although evidence points at intermediate oligomeric species as highly toxic, the accumulation of amyloidogenic plaques would still impede normal homeostasis of the affected tissue from a certain point in time onwards.

FAF Nb1-3 are currently being tested for their ability to prevent 8 kDa AGel fibrillation. With transmission electron microscopy (TEM) and/or atomic-force microscopy (AFM), the differences in fibrillation could then be visualized in order to link reduced toxicity to a specific shift in amyloid oligomerization or fibril species.

Once more Alzheimer's researchers are also exploring this route. Studying the cytotoxic response of SH-SY5Y cells through LDL release, they found that oligomeric Aβ provoked a higher cytotoxic reaction compared to monomeric or fibrillar Aβ [53]. Next, the cells were incubated with oligomeric Aβ formed in the presence of anti-Aβ nanobodies. So far, two distinct nanobodies have been discovered, each binding a specific oligomeric species. Both are able to lower the intrinsic toxicity in SH-SY5Y cells. The first, Nb A4, does so by inhibiting further aggregation of its target. The second, Nb E1, acts in a different manner by binding to smaller Aβ species than Nb A4, thereby interfering earlier in the fibrillation process. Binding its target stabilizes the formation of small non-toxic low-n Aβ species.

It remains to be demonstrated if these approaches and beneficial effects can be translated in model organisms or even in patients, the current findings and results obtained with nanobodies in several amyloid diseases indicate that they could represent an instrument of choice in the diagnosis and/or treatment of these debilitating disorders.

Acknowledgements

This work was supported by the 'Stichting Alzheimer Onderzoek' (SAO-FRA Belgium), the Queen Elisabeth Medical Foundation (GSKE, Belgium) and the Amyloidosis Foundation (USA). A. Verhelle is supported by the Agency for Innovation by Science and Technology in Flanders.

Author details

Adriaan Verhelle and Jan Gettemans*

*Address all correspondence to: jan.gettemans@ugent.be

Department of Biochemistry, Faculty of Medicine and Health Sciences, Ghent University, Ghent, Belgium

http://dx.doi.org/10.5772/63981

References

[1] de la Chapelle A, Tolvanen R, Boysen G, Santavy J, Bleeker-Wagemakers L, Maury CP, et al. Gelsolin-derived familial amyloidosis caused by asparagine or tyrosine substitution for aspartic acid at residue 187. Nature Genetics. 1992;2(2):157–60.

[2] Sethi S, Theis JD, Quint P, Maierhofer W, Kurtin PJ, Dogan A, et al. Renal amyloidosis associated with a novel sequence variant of gelsolin. American Journal of Kidney Diseases: the Official Journal of the National Kidney Foundation. 2013;61(1):161–6.

[3] Efebera YA, Sturm A, Baack EC, Hofmeister CC, Satoskar A, Nadasdy T, et al. Novel gelsolin variant as the cause of nephrotic syndrome and renal amyloidosis in a large kindred. Amyloid: The International Journal of Experimental and Clinical Investigation: the Official Journal of the International Society of Amyloidosis. 2014;21(2):110–2.

[4] Burtnick LD, Urosev D, Irobi E, Narayan K, Robinson RC. Structure of the N-terminal half of gelsolin bound to actin: roles in severing, apoptosis and FAF. The EMBO Journal. 2004;23(14):2713–22.

[5] Chen CD, Huff ME, Matteson J, Page L, Phillips R, Kelly JW, et al. Furin initiates gelsolin familial amyloidosis in the Golgi through a defect in Ca(2+) stabilization. The EMBO Journal. 2001;20(22):6277–87.

[6] Robinson RC, Choe S, Burtnick LD. The disintegration of a molecule: the role of gelsolin in FAF, familial amyloidosis (Finnish type). Proceedings of the National Academy of Sciences of the United States of America. 2001;98(5):2117–8.

[7] Kiuru-Enari S, Haltia M. Hereditary gelsolin amyloidosis. Handbook of Clinical Neurology. 2013;115:659–81.

[8] Van Overbeke W, Verhelle A, Everaert I, Zwaenepoel O, Vandekerckhove J, Cuvelier C, et al. Chaperone nanobodies protect gelsolin against MT1-MMP degradation and alleviate amyloid burden in the gelsolin amyloidosis mouse model. Molecular Therapy: The Journal of the American Society of Gene Therapy. 2014;22(10):1768–78.

[9] Van Overbeke W, Wongsantichon J, Everaert I, Verhelle A, Zwaenepoel O, Loonchanta A, et al. An ER-directed gelsolin nanobody targets the first step in amyloid formation in a gelsolin amyloidosis mouse model. Human Molecular Genetics. 2015;24(9):2492–507.

[10] Meretoja J. Familial systemic paramyloidosis with lattice dystrophy of the cornea, progressive cranial neuropathy, skin changes and various internal symptoms. A previously unrecognized heritable syndrome. Annals of Clinical Research. 1969;1(4):314–24.

[11] Maury CP, Alli K, Baumann M. Finnish hereditary amyloidosis. Amino acid sequence homology between the amyloid fibril protein and human plasma gelsolin. FEBS Letters. 1990;260(1):85–7.

[12] Haltia M, Prelli F, Ghiso J, Kiuru S, Somer H, Palo J, et al. Amyloid protein in familial amyloidosis (Finnish type) is homologous to gelsolin, an actin-binding protein. Biochemical and Biophysical Research Communications. 1990;167(3):927–32.

[13] Kwiatkowski DJ. Functions of gelsolin: motility, signaling, apoptosis, cancer. Current Opinion in Cell Biology. 1999;11(1):103–8.

[14] Silacci P, Mazzolai L, Gauci C, Stergiopulos N, Yin HL, Hayoz D. Gelsolin superfamily proteins: key regulators of cellular functions. Cellular and Molecular Life Sciences: CMLS. 2004;61(19–20):2614–23.

[15] Khurana S, George SP. Regulation of cell structure and function by actin-binding proteins: villin's perspective. FEBS Letters. 2008;582(14):2128–39.

[16] Dominguez R, Holmes KC. Actin structure and function. Annual Review of Biophysics. 2011;40:169–86.

[17] McLaughlin PJ, Gooch JT, Mannherz HG, Weeds AG. Structure of gelsolin segment 1-actin complex and the mechanism of filament severing. Nature. 1993;364(6439):685–92.

[18] Burtnick LD, Koepf EK, Grimes J, Jones EY, Stuart DI, McLaughlin PJ, et al. The crystal structure of plasma gelsolin: implications for actin severing, capping, and nucleation. Cell. 1997;90(4):661–70.

[19] Yin HL, Albrecht JH, Fattoum A. Identification of gelsolin, a Ca2+-dependent regulatory protein of actin gel-sol transformation, and its intracellular distribution in a variety of cells and tissues. The Journal of Cell Biology. 1981;91(3 Pt 1):901–6.

[20] Vouyiouklis DA, Brophy PJ. A novel gelsolin isoform expressed by oligodendrocytes in the central nervous system. Journal of Neurochemistry. 1997;69(3):995–1005.

[21] Choe H, Burtnick LD, Mejillano M, Yin HL, Robinson RC, Choe S. The calcium activation of gelsolin: insights from the 3A structure of the G4-G6/actin complex. Journal of Molecular Biology. 2002;324(4):691–702.

[22] Bucki R, Levental I, Kulakowska A, Janmey PA. Plasma gelsolin: function, prognostic value, and potential therapeutic use. Current Protein & Peptide Science. 2008;9(6):541–51.

[23] Page LJ, Huff ME, Kelly JW, Balch WE. Ca^{2+} binding protects against gelsolin amyloidosis. Biochemical and Biophysical Research Communications. 2004;322(4):1105–10.

[24] Kangas H, Paunio T, Kalkkinen N, Jalanko A, Peltonen L. In vitro expression analysis shows that the secretory form of gelsolin is the sole source of amyloid in gelsolin-related amyloidosis. Human Molecular Genetics. 1996;5(9):1237–43.

[25] Creemers JW, Siezen RJ, Roebroek AJ, Ayoubi TA, Huylebroeck D, Van de Ven WJ. Modulation of furin-mediated proprotein processing activity by site-directed mutagenesis. The Journal of Biological Chemistry. 1993;268(29):21826–34.

[26] Molloy SS, Bresnahan PA, Leppla SH, Klimpel KR, Thomas G. Human furin is a calcium-dependent serine endoprotease that recognizes the sequence Arg-X-X-Arg and efficiently cleaves anthrax toxin protective antigen. The Journal of Biological Chemistry. 1992;267(23):16396–402.

[27] Molloy SS, Thomas L, VanSlyke JK, Stenberg PE, Thomas G. Intracellular trafficking and activation of the furin proprotein convertase: localization to the TGN and recycling from the cell surface. The EMBO Journal. 1994;13(1):18–33.

[28] Kangas H, Seidah NG, Paunio T. Role of proprotein convertases in the pathogenic processing of the amyloidosis-associated form of secretory gelsolin. Amyloid: The International Journal of Experimental and Clinical Investigation: the Official Journal of the International Society of Amyloidosis. 2002;9(2):83–7.

[29] Page LJ, Suk JY, Huff ME, Lim HJ, Venable J, Yates J, et al. Metalloendoprotease cleavage triggers gelsolin amyloidogenesis. The EMBO Journal. 2005;24(23):4124–32.

[30] Kiuru S. Familial amyloidosis of the Finnish type (FAF). A clinical study of 30 patients. Acta Neurologica Scandinavica. 1992;86(4):346–53.

[31] Pihlamaa T, Rautio J, Kiuru-Enari S, Suominen S. Gelsolin amyloidosis as a cause of early aging and progressive bilateral facial paralysis. Plastic and Reconstructive Surgery. 2011;127(6):2342–51.

[32] Page LJ, Suk JY, Bazhenova L, Fleming SM, Wood M, Jiang Y, et al. Secretion of amyloidogenic gelsolin progressively compromises protein homeostasis leading to the intracellular aggregation of proteins. Proceedings of the National Academy of Sciences of the United States of America. 2009;106(27):11125–30.

[33] Kohler G, Milstein C. Continuous cultures of fused cells secreting antibody of predefined specificity. Nature. 1975;256(5517):495–7.

[34] Beck A, Wurch T, Bailly C, Corvaia N. Strategies and challenges for the next generation of therapeutic antibodies. Nature Reviews Immunology. 2010;10(5):345–52.

[35] Hamers-Casterman C, Atarhouch T, Muyldermans S, Robinson G, Hamers C, Songa EB, et al. Naturally occurring antibodies devoid of light chains. Nature. 1993;363(6428):446–8.

[36] Broisat A, Toczek J, Dumas LS, Ahmadi M, Bacot S, Perret P, et al. 99mTc-cAbVCAM1-5 imaging is a sensitive and reproducible tool for the detection of inflamed atherosclerotic lesions in mice. Journal of Nuclear Medicine: Official Publication, Society of Nuclear Medicine. 2014;55(10):1678–84.

[37] Put S, Schoonooghe S, Devoogdt N, Schurgers E, Avau A, Mitera T, et al. SPECT imaging of joint inflammation with Nanobodies targeting the macrophage mannose receptor in a mouse model for rheumatoid arthritis. Journal of Nuclear Medicine: Official Publication, Society of Nuclear Medicine. 2013;54(5):807–14.

[38] Vaneycken I, Devoogdt N, Van Gassen N, Vincke C, Xavier C, Wernery U, et al. Preclinical screening of anti-HER2 nanobodies for molecular imaging of breast cancer. FASEB Journal: Official Publication of the Federation of American Societies for Experimental Biology. 2011;25(7):2433–46.

[39] Dumoulin M, Last AM, Desmyter A, Decanniere K, Canet D, Larsson G, et al. A camelid antibody fragment inhibits the formation of amyloid fibrils by human lysozyme. Nature. 2003;424(6950):783–8.

[40] Pain C, Dumont J, Dumoulin M. Camelid single-domain antibody fragments: uses and prospects to investigate protein misfolding and aggregation, and to treat diseases associated with these phenomena. Biochimie. 2015;111:82–106.

[41] Domanska K, Vanderhaegen S, Srinivasan V, Pardon E, Dupeux F, Marquez JA, et al. Atomic structure of a nanobody-trapped domain-swapped dimer of an amyloidogenic beta2-microglobulin variant. Proceedings of the National Academy of Sciences of the United States of America. 2011;108(4):1314–9.

[42] Rasmussen SG, DeVree BT, Zou Y, Kruse AC, Chung KY, Kobilka TS, et al. Crystal structure of the beta2 adrenergic receptor-Gs protein complex. Nature. 2011;477(7366):549–55.

[43] Dorresteijn B, Rotman M, Faber D, Schravesande R, Suidgeest E, van der Weerd L, et al. Camelid heavy chain only antibody fragment domain against beta-site of amyloid precursor protein cleaving enzyme 1 inhibits beta-secretase activity in vitro and in vivo. The FEBS Journal. 2015;282(18):3618–31.

[44] Vincke C, Loris R, Saerens D, Martinez-Rodriguez S, Muyldermans S, Conrath K. General strategy to humanize a camelid single-domain antibody and identification of a universal humanized nanobody scaffold. The Journal of Biological Chemistry. 2009;284(5):3273–84.

[45] Van Audenhove I, Debeuf N, Boucherie C, Gettemans J. Fascin actin bundling controls podosome turnover and disassembly while cortactin is involved in podosome assembly by its SH3 domain in THP-1 macrophages and dendritic cells. Biochimica et Biophysica Acta. 2015;1853(5):940–52.

[46] Bethuyne J, De Gieter S, Zwaenepoel O, Garcia-Pino A, Durinck K, Verhelle A, et al. A nanobody modulates the p53 transcriptional program without perturbing its functional architecture. Nucleic Acids Research. 2014;42(20):12928–38.

[47] Van den Abbeele A, De Clercq S, De Ganck A, De Corte V, Van Loo B, Soror SH, et al. A llama-derived gelsolin single-domain antibody blocks gelsolin-G-actin interaction. Cellular and Molecular Life Sciences: CMLS. 2010;67(9):1519–35.

[48] Xavier C, Devoogdt N, Hernot S, Vaneycken I, D'Huyvetter M, De Vos J, et al. Site-specific labeling of his-tagged Nanobodies with (9)(9)mTc: a practical guide. Methods in Molecular Biology. 2012;911:485–90.

[49] Conrath KE, Lauwereys M, Galleni M, Matagne A, Frere JM, Kinne J, et al. Beta-lactamase inhibitors derived from single-domain antibody fragments elicited in the camelidae. Antimicrobial Agents and Chemotherapy. 2001;45(10):2807–12.

[50] Wu Z, Yang H, Colosi P. Effect of genome size on AAV vector packaging. Molecular Therapy: the Journal of the American Society of Gene Therapy. 2010;18(1):80–6.

[51] Cecchi C, Stefani M. The amyloid-cell membrane system. The interplay between the biophysical features of oligomers/fibrils and cell membrane defines amyloid toxicity. Biophysical Chemistry. 2013;182:30–43.

[52] Bemporad F, Chiti F. Protein misfolded oligomers: experimental approaches, mechanism of formation, and structure-toxicity relationships. Chemistry & Biology. 2012;19(3):315–27.

[53] Kasturirangan S, Li L, Emadi S, Boddapati S, Schulz P, Sierks MR. Nanobody specific for oligomeric beta-amyloid stabilizes nontoxic form. Neurobiology of Aging. 2012;33(7):1320–8.

IntechOpen